

# Digital Longitudinal Monitoring of Optical Transmission Link

Takeo Sasai

NTT Network Innovation Laboratories, NTT, Yokosuka, Japan, [takeo.sasai.cp@hco.ntt.co.jp](mailto:takeo.sasai.cp@hco.ntt.co.jp)

**Abstract** We review the advancements in Rx DSP-based transmission-link monitoring methods, which reveal fiber-longitudinal distributions of various physical parameters (e.g., signal power profile, gain spectra, and filter responses) along a multi-span link without analog testing instruments. We also discuss the comparison of power profile estimation methods. ©2022 The Author(s)

## Introduction

To operate a transmission system at its maximum rate with less margins, various physical parameters of the link have to be accurately monitored [1]. Numerous studies have been conducted on estimating link parameters such as OSNR, fiber nonlinear noise [2], and polarization mode dispersion [3] from receiver-side (Rx) digital signal processing (DSP). However, these parameters are cumulative information and do not help in estimating the component-wise characteristics or identify the location of anomalies in the link. If *fiber-longitudinal* distribution of link parameters, such as the signal power profile, gain spectrum of each amplifier, and frequency response of each filter, are available, one can

1. predict the transmission performance more accurately by inputting parameters into simulations or design tools (e.g., Gaussian noise models [4],[5],[6]) and select the best transmission modes to maximize the system capacity [7],[8].
2. minimize the margins due to the uncertainty of link-component characteristics [1].
3. automatically localize and sometimes even repair the anomalies in the link (fiber anomaly loss, gain tilts of amplifiers, passband narrowing of filters).

Very recently, digital longitudinal monitoring

(DLM) [9] has been proposed. As shown in Fig. 1, DLM estimates the fiber-longitudinal distributions of various physical characteristics along a multi-span link only from Rx DSP in a digital coherent receiver. Thus far, these characteristics have been measured with analog instruments such as optical time domain reflectometers (OTDR) and optical spectrum analyzers (OSA). Table 1 shows the comparison between these analog approaches and DLM. Though analog approaches provide good measurement accuracy, DLM has the advantages of (i) multi-span measurement, (ii) multi-functionality, and (iii) no need for placing testing instruments on-site.

In this paper, we review DLM in terms of

Table 1 Comparison of analog approaches and DLM

	Analog approach	Digital longitudinal monitoring
Measurement device	Power profile, span-wise CD	OTDR, CD analyzer
	Gain spectrum and tilt	OSA
	Filter responses	OSA
Multi-span measurement	No <sup>2</sup>	Yes (2080 km demonstrated [9,18] <sup>3</sup> )
Dedicated instrument	Required	Not required
On-site measurement	Required (Span by span)	Not required
Others	-	High fiber launch power desired

1: Not necessarily in Rx DSP hardware (processable in a network controller).

2: For OTDR, yes with additional optical configuration.

3: Demonstrated for power profile estimation.

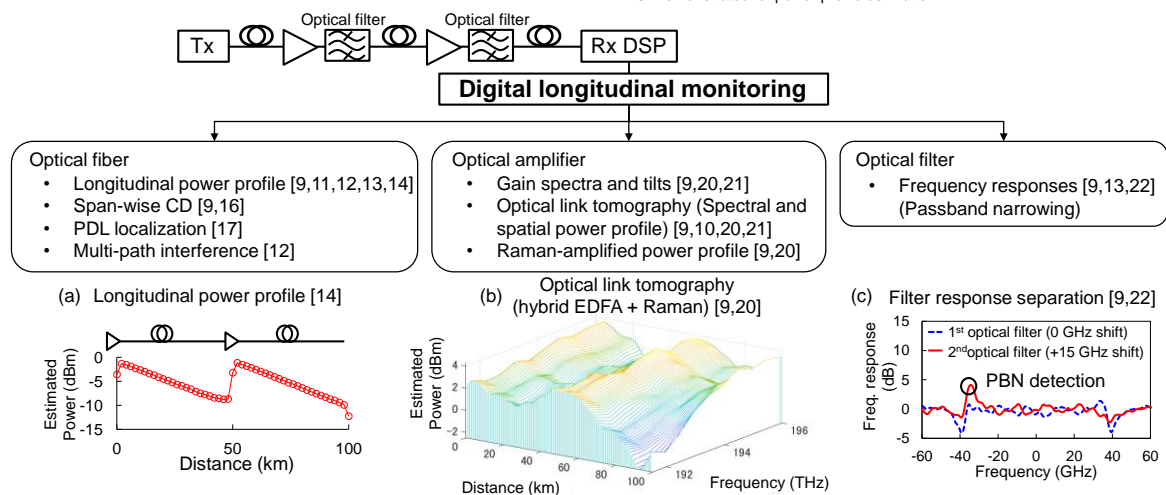


Fig. 1. Digital longitudinal monitoring and its monitored parameters.

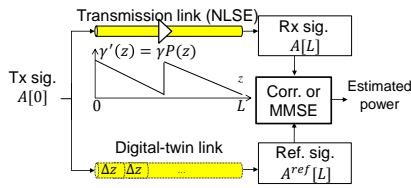


Fig. 2. Common configuration of power profile estimation (PPE) methods. Note that forward propagation of reference signals is assumed.

demonstration experiments, use cases, working principle, and challenges for practical deployment. Comparison of signal power profile estimation (PPE) methods (i.e., correlation-based methods (CMs) [11],[12] and minimum-mean-square-error-based methods (MMSE) [9],[13],[14]) is also conducted.

### Monitored Physical Parameters

#### 1) Optical fiber

The monitored parameters demonstrated thus far are summarized in Fig. 1. The most fundamental technique is fiber-longitudinal signal power profile estimation (PPE) because all the other demonstrations are applications of PPE. As shown Fig. 1(a), PPE reveals the distance-wise signal power distributions. Thus, localization of anomalies in a fiber as well as the amplifier's gain can be monitored over multiple spans. The working principle and comparison of PPE methods are described later. Since the first demonstration of PPE in 2019 [15], span-wise chromatic dispersion (CD) estimation [9],[16], localization of polarization dependent loss (PDL) [17], and multi-path interference [12] have been demonstrated. As an extreme demonstration, power profile over a 2080 km link has successfully been estimated [18]. The theoretical foundation of PPE is provided in [19].

#### 2) Optical amplifier

By obtaining the signal power profile in the wavelength direction using WDM channels, the gain spectrum and tilt of each amplifier can be reconstructed (Fig. 1(b)). The first demonstration was conducted in the context of hybrid Raman + EDFA systems in 2021 [9][20]. After this demonstration, the authors in [10] called this concept optical network tomography (ONT) or OLT since this method unveils signal power in both distance and wavelength cross-sections. In 2022, OLT over C+L bands for EDFA-only systems was demonstrated [21].

#### 3) Optical filters

Localization of anomaly optical filters due to

Table 2 Comparison of PPE methods.

Method	Correlation-based methods (CMs)		Minimum-mean-square-error-based methods (MMSEs)		
	Original CM [11,15]	CM with NL template [12]	Gradient optimization of SSM [9,16]	Volterra [13]	Linear least squares [14]
Digital-twin link model	CD, partial NLPR, residual CD	CD, NL template, residual CD	SSM	Volterra	1st order perturbation
Spatial resolution (see Fig.3)	(Theoretically) Limited <sup>1</sup>	(Theoretically) Limited <sup>1</sup>	(Theoretically) Fine <sup>1</sup>	(Theoretically) Fine <sup>1</sup>	(Theoretically) Fine <sup>1</sup>
Power level diagram estimation in dB	No	Yes <sup>2</sup>	Yes	Yes	Yes
Absolute power estimation	No	No	Yes	Yes	Yes
Random accessibility	Yes	Yes	No	No	No

1: Under noise-less and distortion-less conditions.

2: But a calibration method required (as suggested in [23])

passband narrowing were demonstrated in [9],[13],[22] (Fig. 1(c)). Usually, the frequency responses of two concatenated linear filters cannot be separately estimated since consecutive linear-filter systems are commutative. These methods successfully estimate the filter responses separately by leveraging fiber nonlinearity between the two filters to make the system non-commutative.

### Use Cases

#### 1) Auto optical path provisioning

Since DLM monitors the longitudinal distribution of link parameters, we can predict the transmission performance by inputting them into QoT estimation tools, and select the best transmission modes with less margins [7],[8]. This is useful when establishing a new channel, especially over alien transmission links (e.g., dark fiber).

#### 2) Fault localization

DLM can be used as an anomaly detector to identify the cause of QoT degradation. On the basis of the identified fault, we can take such measures as optimization of fiber launch power, gain equalization, filter passband tuning, and even detouring the anomaly components.

### Working Principle of PPE

PPE estimates the power profile from the nonlinear phase rotation (NLPR) at each position  $z$  on a fiber. The problem of estimating the NLPR can mathematically be regarded as an inverse problem of the nonlinear Schrödinger equation (NLSE) [9], where the nonlinear coefficients

$$\gamma'(z) \equiv \gamma P(z) = \gamma P(0) \exp\left(-\int_0^z \alpha(z') dz'\right)$$

are estimated from boundary conditions (i.e., transmitted signals and received signals). Here,  $P(z)$ ,  $\alpha(z)$ , and  $\gamma$  are signal power, fiber loss, and nonlinear constants, respectively. Since  $\gamma'(z)$  is proportional to  $P(z)$  assuming  $\gamma$  is constant, we can estimate the signal power profile from  $\gamma'(z)$ .

Figure 2 illustrates a common configuration of

PPE methods. The reference (transmitted) signals  $A[0]$  propagate a *digital-twin* link that emulates the actual fiber link (e.g., split-step method, SSM). The digitally propagated reference signals  $A^{ref}[L]$  and received signals  $A[L]$  are then compared to estimate  $\gamma'(z)$  by taking cross-correlation or MMSE.

Note that, though transmitted signals are required for PPE, this does not mean that training or pilot signals are required since transmitted signals can be reconstructed in the receiver by using the standard demodulation process.

### Comparison of PPE methods

Several PPE methods have been proposed (see Table 2) and can be classified into two types: CMs [11],[12] and MMSEs [9],[13],[14]. The differences in these methods are summarized in Table 2. Regarding the algorithms, CMs and MMSEs are different in (i) the model of the digital-twin link and (ii) how the received signals and reference signals are compared (i.e., cross-correlation or MMSE). Also, their performances are fundamentally different as theoretically proven in [19] (we will show this later with a simulation.) MMSEs provide the optimum solution for the inverse problem of NLSE, and thus can achieve significantly high spatial resolution (SR) and estimate the true power in dBm. On the other hand, CMs are a sub-optimal solution: their SR is inherently limited and the true power cannot be estimated. However, CMs are still attractive in terms of their random accessibility and stability.

The original CM proposed by Tanimura et al. [11],[15] uses a partial-NLPR link as the digital-twin link, in which partial CD, partial NLPR  $(\cdot) \exp(j\varepsilon|\cdot|^2)$  at the measurement location, and residual CD are conducted. Here,  $\varepsilon$  is a scaling parameter. Cross-correlations are then taken between  $A^{ref}[L]$  and  $A[L]$ , to estimate  $\gamma'(z)$ . Hahn et al. [12] proposed another CM that uses  $j\varepsilon|\cdot|^2(\cdot)$  instead of  $(\cdot) \exp(j\varepsilon|\cdot|^2)$  to remove an unnecessary power offset accompanying power profiles of the original CM [19].

The original MMSE was proposed in [9][16], with which the power profile is estimated as the optimum  $\gamma'(z)$  of the digital-twin link that minimizes the square error between received signals and reference signals. The original MMSE uses SSM as the digital-twin link and perform gradient descent to optimize SSM coefficients (i.e.,  $\gamma'(z)$ ). The Volterra series expansion was used as another model of a digital-twin link in [13]. For computationally simpler estimation, a linear least squares method was proposed [14].

Figure 3 shows the simulation comparison

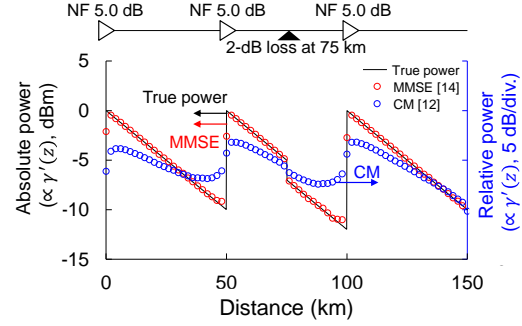


Fig. 3. Comparison of power profile estimated by CM [12] and MMSE [14]. 2-dB attenuation is inserted at 75 km.

between CM and MMSE over  $50 \text{ km} \times 3$  spans using 64QAM 128-GBd signals. While the MMSE showed good agreement with the true power and even estimated the absolute power, CMs had a limited SR and only estimated the relative power even under distortion-less conditions. Since the estimated line of CMs deviates from the true power, a calibration method was proposed [23] for CMs to estimate the correct power change.

### Performance-limiting Factor and Challenges

Since PPE is based on fiber nonlinearity, higher fiber launch power is desirable for enhanced measurement accuracy: otherwise, the NLPR in optical fiber will be contaminated by channel noise (e.g., ASE noise). This is the weakest point of DLM for practical deployment since higher launch power only for a monitored signal is prohibitive in WDM systems. Even so, DLM is useful in a provisioning stage where less signal channels exist in a fiber. From the above discussion, the measurement accuracy at position  $z$  depends on the following nonlinearity-to-noise ratio (NLNR) [9]:

$$\text{NLNR}(z) = \frac{P_{NL}(z)}{N}, \quad (1)$$

where  $P_{NL}(z)$  is the power of nonlinearity within a processed bandwidth at measurement location  $z$  while  $N$  is that of noise at the receiver. However, the effect of  $N$  can be reduced by increasing the signal samples used for cross-correlation or MMSE due to the averaging effect.

Regarding the SR, the amount of CD effect has a significant impact on the SR of CMs. This is because larger CD (walk off) easily collapses the waveform, and the correlation between nonlinearity at a targeted position and a neighboring position becomes lower. Thus, with CMs, a higher baudrate is desirable for SR enhancement. However, the SR of MMSE is not as limited as that of CMs as shown in Fig. 3. This is because MMSE attempt to find NLPR at all positions at the same time while CMs only use a partial NLPR at a single position.

## References

- [1] Y. Pointurier, "Design of Low-Margin Optical Networks," *Journal of Optical Communications and Networking*, vol. 9, no. 1, pp. A9–A17, 2017, DOI: [10.1364/JOCN.9.0000A9](https://doi.org/10.1364/JOCN.9.0000A9)
- [2] Z. Wang, A. Yang, P. Guo, and P. He, "OSNR and nonlinear noise power estimation for optical fiber communication systems using LSTM based deep learning technique", *Optics Express*, vol. 26, no. 16, pp. 21346–21357, 2018, DOI: [10.1364/OE.26.021346](https://doi.org/10.1364/OE.26.021346)
- [3] F. N. Hauske, M. Kuschnerov, B. Spinnler and B. Lankl, "Optical Performance Monitoring in Digital Coherent Receivers," *Journal of Lightwave Technology*, vol. 27, no. 16, pp. 3623-3631, 2009, DOI: [10.1109/JLT.2009.2024960](https://doi.org/10.1109/JLT.2009.2024960)
- [4] A. Carena, G. Bosco, V. Curri, Y. Jiang, P. Poggiolini, and F. Forghieri, "EGN model of non-linear fiber propagation," *Optics Express*, vol. 22, no. 13, pp. 16335–16362, 2014, DOI: [10.1364/OE.22.016335](https://doi.org/10.1364/OE.22.016335)
- [5] P. Serena and A. Bononi, "A Time-Domain Extended Gaussian Noise Model," *Journal of Lightwave Technology*, vol. 33, no. 7, pp. 1459-1472, 2015, DOI: [10.1109/JLT.2015.2398873](https://doi.org/10.1109/JLT.2015.2398873)
- [6] A. Ferrari, M. Filer, K. Balasubramanian, Y. Yin, E. L. Rouzic, J. Kundrat, G. Grammel, G. Galimberti, and V. Curri, "GNPy: an open source application for physical layer aware open optical networks," *Journal of Optical Communications and Networking*, vol. 12, no. 6, pp. C31-C40, 2020, DOI: [10.1364/JOCN.382906](https://doi.org/10.1364/JOCN.382906)
- [7] B. Spinnler, A. X. Lindgren, U. Andersen, S. Melin, J. Slovak, W. Schairer, K. Pulverer, J. Mårtensson, E. D. Man, G. Khanna, R. H. Derksen, J. Steinmayer, R. Jozapovics, J. Blume, T. Lemström, J. Christensen, U. Häbel, U. Bauer, A. Napoli, and B. Sommerkorn-Krombholz, "Autonomous intelligent transponder enabling adaptive network optimization in a live network field trial," *Journal of Optical Communications and Networking*, vol. 11, no. 9, pp. C1-C9, 2019, DOI: [10.1364/JOCN.11.0000C1](https://doi.org/10.1364/JOCN.11.0000C1)
- [8] K. Anazawa, S. Kuwabara, T. Sasai, T. Mano, T. Inoue, T. Inui, and H. Nishizawa, "Automatic Modulation-Format Selection with White-box Transponders: Design and Field Trial," *OptoElectronics and Communications Conference*, 2021, JS2A.14, DOI: [10.1364/OECC.2021.JS2A.14](https://doi.org/10.1364/OECC.2021.JS2A.14)
- [9] T. Sasai, M. Nakamura, E. Yamazaki, S. Yamamoto, H. Nishizawa and Y. Kisaka, "Digital Longitudinal Monitoring of Optical Fiber Communication Link," *Journal of Lightwave Technology*, vol. 40, no. 8, pp. 2390-2408, 2022, DOI: [10.1109/JLT.2021.3139167](https://doi.org/10.1109/JLT.2021.3139167)
- [10] T. Tanimura, S. Yoshida, K. Tajima, S. Oda, and T. Hoshida, "Concept and implementation study of advanced DSP-based fiber-longitudinal optical power profile monitoring toward optical network tomography," *Journal of Optical Communications and Networking*, vol. 13, no. 10, E132-E141, 2021, DOI: [10.1364/JOCN.425494](https://doi.org/10.1364/JOCN.425494)
- [11] T. Tanimura, S. Yoshida, K. Tajima, S. Oda and T. Hoshida, "Fiber-Longitudinal Anomaly Position Identification Over Multi-Span Transmission Link Out of Receiver-end Signals," *Journal of Lightwave Technology*, vol. 38, no. 9, pp. 2726-2733, 2020, DOI: [10.1109/JLT.2020.2984270](https://doi.org/10.1109/JLT.2020.2984270)
- [12] C. Hahn, J. Chang, and Z. Jiang, "Localization of reflection Induced multi-path-interference over multi-span transmission link by receiver-side digital signal processing," *Optical Fiber Communications Conference and Exhibition*, Th1C.3, 2022, DOI: [10.1364/OFC.2022.Th1C.3](https://doi.org/10.1364/OFC.2022.Th1C.3)
- [13] S. Gleb, P. Konstantin, J. Luo, and B. Zheng, "Fiber link anomaly detection and estimation based on signal nonlinearity," *European Conference on Optical Communication*, Tu2C2.5, 2021. DOI: [10.1109/ECOC52684.2021.9606094](https://doi.org/10.1109/ECOC52684.2021.9606094)
- [14] T. Sasai, E. Yamazaki, M. Nakamura, and Y. Kisaka, "Proposal of linear least squares for fiber-nonlinearity-based longitudinal power monitoring in multi-span link," *OptElectronics and Communications Conference*, WB3-1, 2022. DOI: [10.23919/OECC/PSC53152.2022.9850175](https://doi.org/10.23919/OECC/PSC53152.2022.9850175)
- [15] T. Tanimura, K. Tajima, S. Yoshida, S. Oda and T. Hoshida, "Experimental demonstration of a coherent receiver that visualizes longitudinal signal power profile over multiple spans out of its incoming signal," *European Conference on Optical Communication*, PD.3.4, 2019, DOI: [10.1049/cp.2019.1031](https://doi.org/10.1049/cp.2019.1031)
- [16] T. Sasai, M. Nakamura, S. Okamoto, F. Hamaoka, S. Yamamoto, E. Yamazaki, A. Matsushita, H. Nishizawa, and Y. Kisaka, "Simultaneous detection of anomaly points and fiber types in multi-span transmission links only by receiver-side digital signal processing," *Optical Fiber Communications Conference and Exhibition*, Th1F.1, 2020, DOI: [10.1364/OFC.2020.Th1F.1](https://doi.org/10.1364/OFC.2020.Th1F.1)
- [17] M. Eto, K. Tajima, S. Yoshida, S. Oda, and T. Hoshida, "Location-resolved PDL monitoring with Rx-side digital signal processing in multi-span optical transmission system," *Optical Fiber Communications Conference and Exhibition*, Th1C.2, 2022, DOI: [10.1364/OFC.2022.Th1C.2](https://doi.org/10.1364/OFC.2022.Th1C.2)
- [18] T. Sasai, M. Nakamura, E. Yamazaki and Y. Kisaka, "Precise Longitudinal Power Monitoring over 2,080 km Enabled by Step Size Selection of Split Step Fourier Method," *Optical Fiber Communications Conference and Exhibition*, Th1C.4, 2022, DOI: [10.1364/OFC.2022.Th1C.4](https://doi.org/10.1364/OFC.2022.Th1C.4)
- [19] T. Sasai, E. Yamazaki, M. Nakamura, and Y. Kisaka, "Closed-Form Expressions for Fiber-Nonlinearity-Based Longitudinal Power Profile Estimation Methods," *European Conference on Optical Communication*, Tu1D.6, 2022.
- [20] T. Sasai, M. Nakamura, T. Kobayashi, H. Kawakami, E. Yamazaki and Y. Kisaka, "Revealing Raman-amplified Power Profile and Raman Gain Spectra with Digital Backpropagation," *Optical Fiber Communications Conference and Exhibition*, M3I.5, 2021, DOI: [10.1364/OFC.2021.M3I.5](https://doi.org/10.1364/OFC.2021.M3I.5)
- [21] M. R. Sena, R. Emmerich, B. Shariati, J. K. Fischer, and R. Freund, "Link Tomography for Amplifier Gain Profile Estimation and Failure Detection in C+L-band Open Line Systems," *Optical Fiber Communications Conference and Exhibition*, Th1H.1, 2022, DOI: [10.1364/OFC.2022.Th1H.1](https://doi.org/10.1364/OFC.2022.Th1H.1)
- [22] T. Sasai, M. Nakamura, E. Yamazaki, S. Yamamoto, H. Nishizawa and Y. Kisaka, "Digital Backpropagation for Optical Path Monitoring: Loss Profile and Passband Narrowing Estimation," *European Conference on Optical Communications*, Tu2D. 1, 2020, DOI: [10.1109/ECOC48923.2020.9333191](https://doi.org/10.1109/ECOC48923.2020.9333191)
- [23] A. May, F. Boitier, E. Awwad, P. Ramantanis, M. Lonardi, and P. Ciblat, "Receiver-based experimental estimation of power losses in optical networks," *IEEE Photonics Technology Letters*, vol. 33, no. 22, pp. 1238–1241, 2021. DOI: [10.1109/LPT.2021.3115627](https://doi.org/10.1109/LPT.2021.3115627).